

# The effects of residual $\alpha$ phase on the 1370 °C creep performance of yttria-doped HIPed silicon nitride

A. A. WERESZCZAK, T. P. KIRKLAND, M. K. FERBER, T. R. WATKINS  
*High Temperature Materials Laboratory, Oak Ridge National Laboratory, Oak Ridge,  
 TN 37831, USA*

R. L. YECKLEY  
*Northboro Research and Development Center, Saint-Gobain/Norton Industrial Ceramics  
 Corporation, Northboro, MA 01532, USA*  
*E-mail: wereszczaka@ornl.gov*

The creep behaviour at 1370 °C (2500 °F) of yttria-doped, hot isostatically pressed silicon nitride was examined as a function of residual  $\alpha$  phase content. The pre-test silicon nitride materials had either 30% or 40%  $\alpha$  phase content. The creep resistance was found to increase as the residual  $\alpha$  phase content decreased. For equivalent times and stresses, the higher  $\alpha$ -containing silicon nitride accumulated more creep strain and exhibited faster creep rates. The residual  $\alpha$  phase decreased as a function of time at 1370 °C and converted to  $\beta$  phase; it was also found that the  $\alpha$  to  $\beta$  phase transformation rate was enhanced by stress. In the absence of stress, the kinetics of the  $\alpha$  to  $\beta$  phase transformation at 1370 °C followed a first-order reaction. If a first-order reaction was assumed for the  $\alpha$  to  $\beta$  phase transformation in the presence of stress at 1370 °C, then the magnitude of the reaction rate constant for this transformation was twice as large for tensile stresses equal to or greater than 130 MPa than for the reaction rate constant describing the transformation with no applied stress. © 1998 Chapman & Hall

## 1. Introduction

Silicon nitride ( $\text{Si}_3\text{N}_4$ ), silicon carbide, and several types of ceramic matrix composites are being considered for component applications in advanced gas turbine engines. Silicon nitride, though, has emerged as the leading candidate for the components subjected to the highest temperatures due to its unique combination of properties including good chemical inertness, desired strength, good creep resistance at 1370 °C with modestly high stresses, and relatively high Weibull modulus. Great efficiency and economy may be attained at a turbine inlet temperature at 1370 °C (2500 °F), so there is a desire to achieve this operating temperature. For example, engine horsepower may be doubled while fuel economy is increased by as much as 20% compared to a similar-sized all-metallic engine [1].

The creep performance of  $\text{Si}_3\text{N}_4$  at 1370 °C has been the focus of many studies over the years, and its creep behaviour has been attributed to mechanisms associated with the grain-boundary secondary phase. Ferber and Jenkins [2] observed anomalously poor creep resistance for  $\text{Si}_3\text{N}_4$  that had incomplete secondary-phase crystallization. Menon *et al.* [3] observed both two-grain (the two-grain cavitation process involves the dissolution of  $\text{Si}_3\text{N}_4$  from grains into the grain boundaries) and multi-grain junction cavities resulting as a consequence of creep of  $\text{Si}_3\text{N}_4$  at

1371 °C. This process occurs more rapidly in silicon nitrides that have higher cation impurity content in their grain boundaries [4], and the creep resistance at 1370 °C suffers as a consequence. Lastly, it was shown by Ferber *et al.* [5] that improved creep resistance in  $\text{Si}_3\text{N}_4$  at 1370 °C was associated with inhibited two-grain cavitation. In each of these cases, the manipulation (or lack thereof) of secondary-phase associated phenomena affected the creep performance of  $\text{Si}_3\text{N}_4$ .

Apart from creep performance differences associated with the secondary phases in  $\text{Si}_3\text{N}_4$ , differences in creep performance of  $\text{Si}_3\text{N}_4$  have been observed to be associated with changes in the primary  $\text{Si}_3\text{N}_4$  phase as well; in particular, changes associated with the residual  $\alpha$ - $\text{Si}_3\text{N}_4$  phase content. Firstly, in previous studies by the authors (see Fig. 1) [3, 4, 6], the fraction of remaining  $\alpha$ - $\text{Si}_3\text{N}_4$  to  $\beta$ - $\text{Si}_3\text{N}_4$  in fact decreased during creep tests at 1370 °C for three different hot isostatically pressed (HIPed)  $\text{Si}_3\text{N}_4$  materials. Also, the static creep resistance of a HIPed  $\text{Si}_3\text{N}_4$  at 125 MPa and 1370 °C improved if the specimen was first subjected to reverse cyclic loading at 1370 °C at 1 Hz for approximately  $1.5 \times 10^6$  cycles (or 410 h) [7], which is illustrated in Fig. 2. In addition to the improvement in creep resistance, the as-received grain structure of the  $\text{Si}_3\text{N}_4$ , Fig. 3a significantly changed as a consequence of cyclic loading, see Fig. 3b

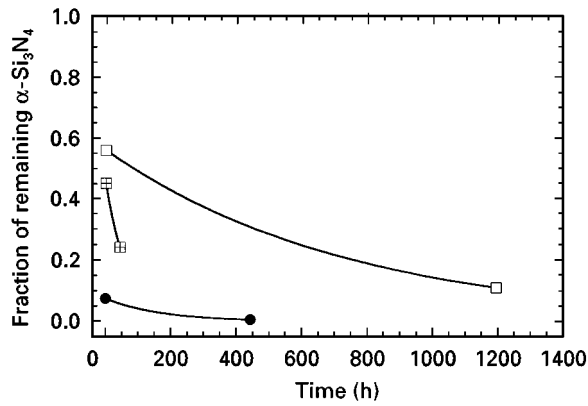


Figure 1 In previous studies by the authors, the fraction of remaining  $\alpha$ - $\text{Si}_3\text{N}_4$  decreased for three different HIPed materials as a consequence of creep testing at  $1370^\circ\text{C}$ . First-order reaction kinetics (—) were assumed, after Bowen *et al.* [11], for (●) NT154 (145 MPa) [3], (□) NT164 (150 MPa) [6], (■) NCX-5102 (140 MPa) [4].

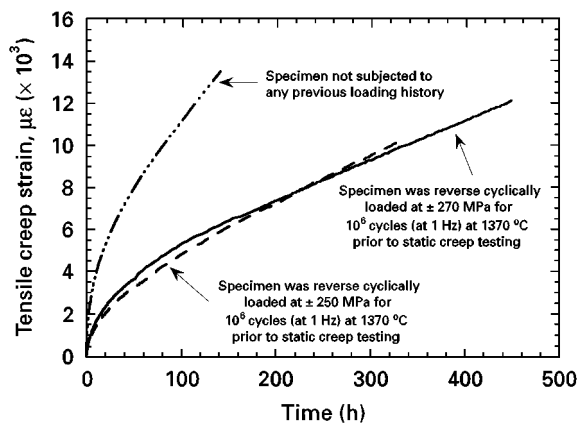


Figure 2 In a previous study [7], the static creep resistance of a HIPed silicon nitride at 125 MPa and  $1370^\circ\text{C}$  improved if the specimen was first subjected to reverse cyclic loading at  $1370^\circ\text{C}$  at 1 Hz for approximately  $1.5 \times 10^6$  cycles (or 410 h).

[7]. Lastly, preliminary results showed the  $\alpha$  phase in a HIPed  $\text{Si}_3\text{N}_4$  decreased more rapidly with the combination of stress and time (reverse cyclic loading at 1 Hz for approximately  $1.5 \times 10^6$  cycles or 410 h at  $1370^\circ\text{C}$ ) versus *just* exposure time, as shown in Fig. 4 [7].

It was not understood in these previous studies whether (1) the reduction in  $\alpha$  phase content, (2) the improved creep resistance at  $1370^\circ\text{C}$  that occurred after cyclic loading at  $1370^\circ\text{C}$ , or (3) the  $\text{Si}_3\text{N}_4$  grain structure changes, were a consequence of *just* exposure at  $1370^\circ\text{C}$  or a synergistic effect that was a consequence of *both* time and stress. The motive behind the present study was to examine these effects more systematically and attempt to explain and link their activities.

## 2. The $\alpha$ to $\beta$ phase transformation in $\text{Si}_3\text{N}_4$

The transformation of the  $\alpha$ - $\text{Si}_3\text{N}_4$  phase to the  $\beta$ - $\text{Si}_3\text{N}_4$  phase is well documented. The majority of studies involving the transformation have been conducted with hot-pressed MgO-doped  $\text{Si}_3\text{N}_4$  systems at temperatures in excess of  $1400^\circ\text{C}$ . The

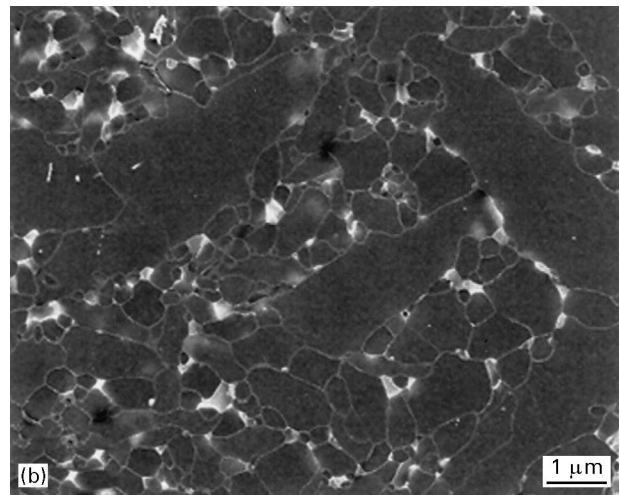
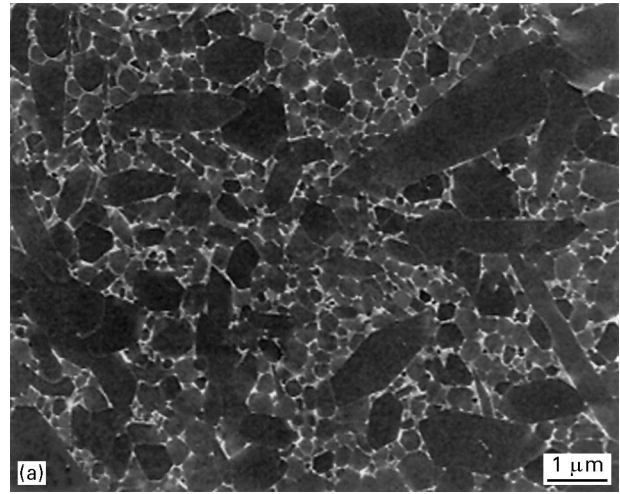


Figure 3 In a previous study [7], the grain structure of a HIPed silicon nitride significantly changed as a consequence of reverse cyclic loading at  $1370^\circ\text{C}$  at 1 Hz for approximately  $1.5 \times 10^6$  cycles (or 410 h). Representative secondary electron images shows the changed grain structure in (a) compared to the as-received microstructure in (b).

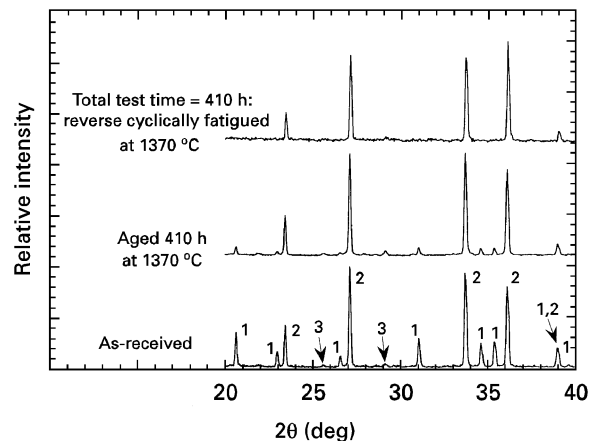


Figure 4 From preliminary findings in a previous study [7], the  $\alpha$  phase in a HIPed silicon nitride decreased more rapidly with the combination of stress and time (reverse cyclic loading at 1 Hz for approximately  $1.5 \times 10^6$  cycles or 410 h at  $1370^\circ\text{C}$ ) versus *just* exposure time, 1,  $\alpha$ - $\text{Si}_3\text{N}_4$  (9–250); 2,  $\beta$ - $\text{Si}_3\text{N}_4$  (33–1160); 3,  $\gamma$ - $\text{Y}_2\text{Si}_2\text{O}_7$  (32–1448). The numbers refer to JCPDS card numbers.

transformation mechanism is the same for HIPed  $\text{Y}_2\text{O}_3$ -doped  $\text{Si}_3\text{N}_4$  but the transformation rate is likely to be much slower in  $\text{Y}_2\text{O}_2$ -doped  $\text{Si}_3\text{N}_4$  than

MgO-doped Si<sub>3</sub>N<sub>4</sub> at equivalent temperatures. The secondary phases, yttrium–silicon oxynitrides, are more refractory (or viscous) than magnesium–silicon oxynitrides because the eutectic temperature for the magnesium–silicon oxynitride is approximately 100 °C lower than that for the yttrium–silicon oxynitride [8]. This is further refelcted by the better high-temperature mechanical performances of the Y<sub>2</sub>O<sub>3</sub>-doped Si<sub>3</sub>N<sub>4</sub> reported by Wiederhorn and Tighe [9]. The α and β phases are both hexagonal with the α phase unit cell (Si<sub>12</sub>N<sub>16</sub>) being about twice as large as the β phase (Si<sub>6</sub>N<sub>8</sub>). The transformation of α to β occurs via a solution–precipitation (solid/liquid/solid) mechanism, and it has been reported that α and β are probably low- and high-temperature forms, respectively [10]. In practice, the transformation of α to β occurs during hot-pressing or hot isostatically pressing (HIPing), mainly after the completion of densification [11]. The transformation mechanism involves the transport of silicon and nitrogen from α grains through a silicate liquid phase to nucleation sites for β at α/liquid interfaces or to β grains nucleated homogeneously in the liquid phase [12]. In practice, it has been recognized that α-Si<sub>3</sub>N<sub>4</sub> can be densified more readily than the β phase. The grain structures of dense ceramics prepared from low β starting material appear more uniform and more fibrous than those of high β starting material [12].

Several parameters affect the rate or the kinetics of the α-Si<sub>3</sub>N<sub>4</sub> to β-Si<sub>3</sub>N<sub>4</sub> transformation. Increasing the hot-pressing pressure increases the transformation rate of α to β [13], which is a consequence of the enhanced nucleation rate of β. A fine, uniform, microstructure with good mechanical strength is typically produced; however, if hot-pressing time is extended beyond that required for α to β conversion, coarsening of the β grains will degrade mechanical properties [13]. The conversion of α to β occurs in MgO-sintered Si<sub>3</sub>N<sub>4</sub> in the absence of stress, but it has been reported that Y<sub>2</sub>O<sub>3</sub>-sintered Si<sub>3</sub>N<sub>4</sub> requires the application of stress to enhance the transformation [10]. (As will be shown, the ageing results for the Y<sub>2</sub>O<sub>3</sub>-doped Si<sub>3</sub>N<sub>4</sub> examined in the present study contradict this.) Impurities (e.g. alkaline and alkaline-earth cations, and transition metal cations) enhance the solution of the α phase because they act to reduce the liquidus temperature and increase the volume of liquid [12]. For MgO-doped Si<sub>3</sub>N<sub>4</sub>, the rate increases with the quantity of additive and with an increase in temperature [11]; the same trend is believed to hold true for Y<sub>2</sub>O<sub>3</sub>-doped Si<sub>3</sub>N<sub>4</sub>.

The kinetics of the α to β transformation, the majority of which occurs after densification is complete, has been shown to be well-described [11] by a first-order reaction

$$d\alpha/dt = -K\alpha \quad (1)$$

where α represents the amount of α phase and K is a reaction rate constant. The solution to this differential equation is

$$\ln(\alpha) = -Kt \quad (2)$$

By plotting the logarithm of α on the ordinate axis as a function of linear time, the identification of a

first-order reaction (i.e. a straight line through the data) may be made. A linear–linear representation of first-order reactions for the transformation of α phase to β phase was shown in Fig. 1.

Perhaps there are two reasons why no literature was found that described the reaction rate kinetics of the α to β transformation in Y<sub>2</sub>O<sub>3</sub>-doped Si<sub>3</sub>N<sub>4</sub> at temperatures as low as 1370 °C. Firstly, it has been long established that heat treatments of α-Si<sub>3</sub>N<sub>4</sub> at temperatures in excess of 1500 °C convert it to β-Si<sub>3</sub>N<sub>4</sub> during processing [14]. Secondly, many of the yttrium–silicon oxynitride phases form at eutectic temperatures at 1500 °C and above [8, 15]. It would not have been relevant for developers of Y<sub>2</sub>O<sub>3</sub>-doped Si<sub>3</sub>N<sub>4</sub> to examine any transformation kinetics at 1370 °C because sintering and transformation conditions occur at temperatures far in excess of 1370 °C. However, the α to β phase transformation will be shown to proceed at 1370 °C in the present study, albeit much more sluggishly than it likely occurred during HIPing.

### 3. Experimental procedure

#### 3.1. NT164 silicon nitride

The material examined in this study was a commercially available HIPed Y<sub>2</sub>O<sub>3</sub>-doped silicon nitride, NT164 (Saint-Gobain/Norton Industrial Ceramic Company, Northboro, MA). Some of the high-temperature mechanical properties of NT164 have been reported [5, 16, 17]. The starting Si<sub>3</sub>N<sub>4</sub> powder (Ube Industries Ltd, Tokyo, Japan) contained more than 95 vol % of the α phase; 4 wt % yttria (Y<sub>2</sub>O<sub>3</sub>) was added as a sintering aid. Using theoretical densities of 3.44 and 5.01 g cm<sup>-3</sup> for Si<sub>3</sub>N<sub>4</sub> and Y<sub>2</sub>O<sub>3</sub>, respectively, a rule of mixtures calculation shows this 4 wt % Y<sub>2</sub>O<sub>3</sub> to be 2.8 vol %. The composition of NT164 lies slightly above the Si<sub>3</sub>N<sub>4</sub> and Y<sub>2</sub>Si<sub>2</sub>O<sub>7</sub> tie-line within the so-called Si<sub>3</sub>N<sub>4</sub>–Si<sub>2</sub>N<sub>2</sub>O–Y<sub>2</sub>Si<sub>2</sub>O<sub>7</sub> compatibility triangle. Strength and oxidation resistance are reportedly maximized in the composition regime in which NT164 resides [18]. The powder mixture was cold isostatically pressed at 207 MPa (30 × 10<sup>3</sup> p.s.i.) into rod blanks, glass-encapsulated, then HIPed using a proprietary temperature–time cycle. The HIPing cycle was controlled to (1) promote grain-boundary crystallization which has been shown in many studies to improve mechanical performance [18–23] and (2) produce NT164 having 30% or 40% residual α phase contents. The X-ray diffraction profiles for these two grades of as-received NT164 are shown in Fig. 5 and show the α phase contents and secondary phases. Cylindrical button-head tensile specimens (6.35 mm diameter and 35 mm gauge length) were machined. Specimens were subjected to a post-machining heat treatment to promote “oxidation-healing” of any machining flaws.

#### 3.2. Creep and ageing testing

Button-head tensile specimens with 30 and 40 vol % (designated in the present study as “low” and “high”

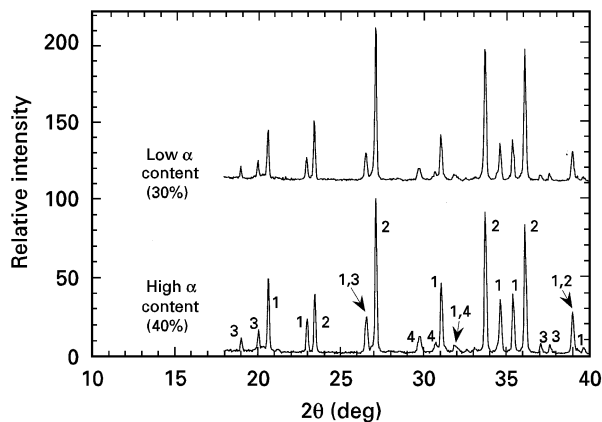


Figure 5 X-ray diffraction results showed that the two grades of NT164 silicon nitride that were creep tested has as-received  $\alpha$  phase contents of 30% or 40%. Trace amounts of secondary phases of  $\text{Si}_2\text{N}_2\text{O}$  and  $\alpha\text{-Y}_2\text{Si}_2\text{O}_7$  also were identified in both grades of the as-received materials. 1,  $\alpha\text{-Si}_3\text{N}_4$  (9–250); 2,  $\beta\text{-Si}_3\text{N}_4$  (33–1160); 3,  $\text{Si}_2\text{N}_2\text{O}$  (18–1171); 4,  $\alpha\text{-Y}_2\text{Si}_2\text{O}_7$  (38–0223). The numbers refer to JCPDS card numbers.

$\alpha$  contents, respectively) residual  $\alpha$ -phase composition were creep-ruptured at 1370 °C at 130 and 150 MPa in ambient air (40%–60% RH, 25 °C). The test hardware has been described elsewhere [2–5]. Briefly, electro-mechanical tensile test machines in electronic closed-loop load control were used for the mechanical loading (Model 1380, Instron Corp., Canton, MA). Specimen grips were positioned outside a compact two-zone resistance-heated furnace. The grips were attached to the load frame in series with hydraulic couplers that were tensile-load activated and designed to minimize specimen bending. Oxygen-free copper collets interfaced the couplers and specimen. With properly activated hydraulic couplers and accurate specimen and collet machining, bending at the examined creep stresses was less than 5% [2]. Creep strain was measured using a high-temperature contact extensometer having a 25 mm gauge length. A computer was used for data acquisition; test load, load error from setpoint, temperature, and extensometer displacement were monitored as a function of time until specimen failure.

An ageing study (time at temperature with no applied stress) on NT164 was performed at 1370 °C. Three discs (about 3 mm thick and 16 mm diameter) of NT164 were set in a furnace and aged at 1370 °C in ambient air (40%–60% RH, 25 °C). One specimen was removed at intermittent times (150 and 400 h) with the final disc removed after the same duration that an NT164 specimen had creep-ruptured (815 h).

### 3.3. Post-testing material analysis

The post-testing material analysis included phase identification using X-ray diffraction (XRD) and microstructural examination using scanning electron microscopy (SEM). The changes in the NT164 material that was creep-ruptured were compared with those in the NT164 material that was aged. The specimens subjected to XRD analysis were scanned at a rate of 1° min<sup>-1</sup> with Cu K<sub>α</sub> radiation ( $\lambda = 0.154$  nm). The

power level of the generator was 1.8 kW (45 kV and 40 mA). A continuous scan mode was employed with a step size of 0.02° over a 2 $\theta$  range of 10°–120°. However, graphical analysis was only performed in the range of 18° < 2 $\theta$  < 40° because the peak and profile information of interest for the  $\text{Si}_3\text{N}_4$  existed in this range. Samples were mounted on the goniometer using putty and a “C” channel offset spacer such that the surface of interest was flush with the fiducial surface in the spring-loaded sample holder. The entire cross-section of the samples was irradiated such that information from the distinct surface and bulk regions should be present. Primary and secondary phases sought were those comprising the  $\text{Y}_2\text{O}_3\text{-SiO}_2\text{-Si}_3\text{N}_4$  system, with emphasis on those phases in compatibility triangles in, and adjacent to,  $\text{Si}_3\text{N}_4\text{-Y}_2\text{Si}_2\text{O}_7\text{-Si}_2\text{N}_2\text{O}$  pseudo-ternary system. Quantitative XRD analysis of the fractions of the  $\alpha$ - and  $\beta\text{-Si}_3\text{N}_4$  phases was conducted using the analysis of Devlin and Amin [24].

The grain structures of the  $\text{Si}_3\text{N}_4$  were examined on polished, plasma-etched surfaces using secondary electron imaging (SEI) with the SEM. Carbon tetrafluoride ( $\text{CF}_4$ ) plasma-etching was performed for 4 min to help distinguish adjacent grains on the polished surfaces. The minimum required time of 4 min for sufficiently plasma-etching the NT164 microstructure was longer than that of similar materials with greater volume fractions of secondary phase (e.g.  $\text{SiAlON}$  and a reported etching time of 1 min [25]). The advantage of this etching process is that  $\text{CF}_4$  etchant preferentially attacks the  $\text{Si}_3\text{N}_4$  grains while not altering the secondary phase. With the secondary phase only comprising 2.8 vol % of the NT164, the grain boundaries were very thin and difficult to discern at two-grain junctions, so contrast-enhancement via  $\text{CF}_4$  plasma etching was required for any constructive SEM examination.

## 4. Results and discussion

### 4.1. Creep performance

A higher amount of residual  $\alpha$  phase in the NT164 resulted in poorer creep resistance. For equivalent times and stresses, the  $\text{Si}_3\text{N}_4$  having a higher  $\alpha$  phase content accumulated more creep strain and exhibited a faster creep rate, as illustrated by Fig. 6. The applied stress, lifetime, creep strain to failure, and minimum creep rate for each of these four specimens are listed in Table I. Only one (low  $\alpha$  – 130 MPa) of the four creep-strain profiles exhibited tertiary creep while all profiles exhibited a steady-state creep regime up to their strain to failure.

Similar creep strain profiles were reported by Ferber *et al.* [5] for creep tests on a slightly older vintage of NT164 at 1370 °C. For the familiar Norton–Bailey equation, a creep stress exponent of 3.3, a pre-exponential value of  $5.82 \times 10^{15}$ , and an activation energy of 795 kJ mol<sup>-1</sup> were reported for this older vintage of NT164. Using these values for creep tests for the later vintage of NT164 examined in the present study, minimum creep rates for 130 and 150 MPa are calculated to be 2.9 and  $4.7 \times 10^{-9}$  s<sup>-1</sup>, which are

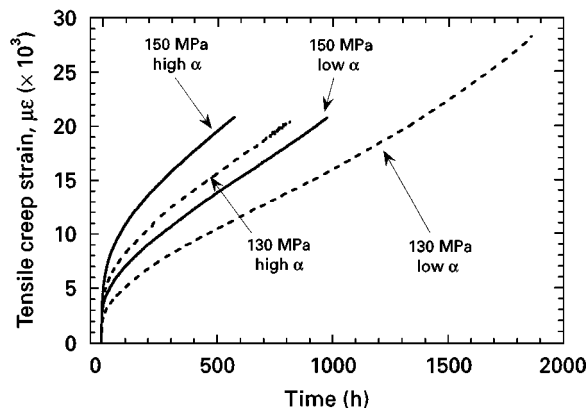


Figure 6 For any equivalent stress and time at 1370 °C, the NT164 silicon nitride containing more  $\alpha$  phase had accumulated more creep strain and exhibited a faster creep rate.

TABLE I Values of engineering creep parameters for tests conducted at 1370 °C

$\alpha$ content	Stress (MPa)	Time to failure (h)	Creep strain to failure ( $\mu\epsilon$ )	Minimum creep rate ( $10^{-9} \text{ s}^{-1}$ )
Low	130	1864	28310	3.1
Low	150	976	20770	3.9
High	130	815	20380	4.3
High	150	575 <sup>a</sup>	20820 <sup>a</sup>	4.8 <sup>a</sup>

<sup>a</sup> Test interrupted because of equipment malfunction and was not tested to failure; shown value likely not the same if the test had continued unaltered.

statistically equivalent to the experimentally determined values.

Because the NT164 materials in this study were subjected to a secondary-phase crystallization heat treatment as part of the HIPing cycle, the change from primary to steady-state creep is not explained by a time-dependent devitrification (or “hardening”) effect during the early duration of creep. The transition to steady-state creep may arise from greater frequency of grain to grain contacts with continued grain-boundary sliding. However, an additional mechanism or explanation may be the time- (and stress) dependent  $\alpha$  to  $\beta$  transformation that is occurring, and the alteration of the grain structure that occurs as a consequence. Evidence of this phenomenon follows.

## 4.2. Analysis of material changes

### 4.2.1. $\alpha$ and $\beta$ phase change

The  $\alpha$  phase content was found to decrease as a function of time and its transformation to  $\beta$  was additionally increased with the application of stress. For identifying the qualitative amount of  $\alpha$ - $\text{Si}_3\text{N}_4$ , it is most convenient to examine the intensity of the X-ray peaks at a  $2\theta$  of approximately  $34.6^\circ$  or  $35.4^\circ$ . The three diffraction patterns in Fig. 7 show the reduction of  $\alpha$  phase through 815 h. The amount of the secondary phases does not significantly change, and only the  $\alpha$  phase content appears to change

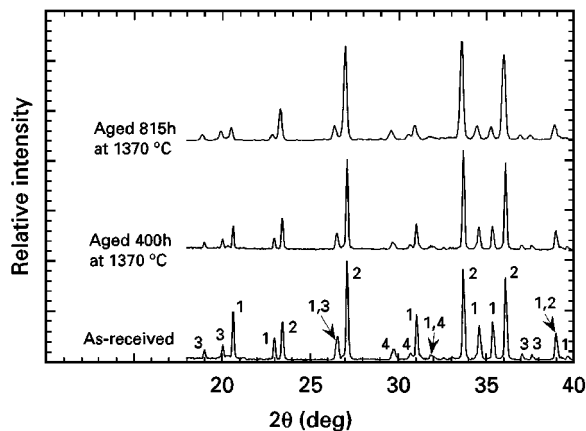


Figure 7 The X-ray diffraction profiles from materials that were aged at 1370 °C without applied stress showed a gradual decrease in the  $\alpha$  phase content as a function of ageing time. There were no significant changes in the secondary phases as a function of ageing time. 1,  $\alpha$ - $\text{Si}_3\text{N}_4$  (9–250); 2,  $\beta$ - $\text{Si}_3\text{N}_4$  (33–1160); 3,  $\text{Si}_2\text{N}_2\text{O}$  (18–1171); 4,  $\alpha$ - $\text{Y}_2\text{Si}_2\text{O}_7$  (38–0223). The numbers refer to JCPDS card numbers.

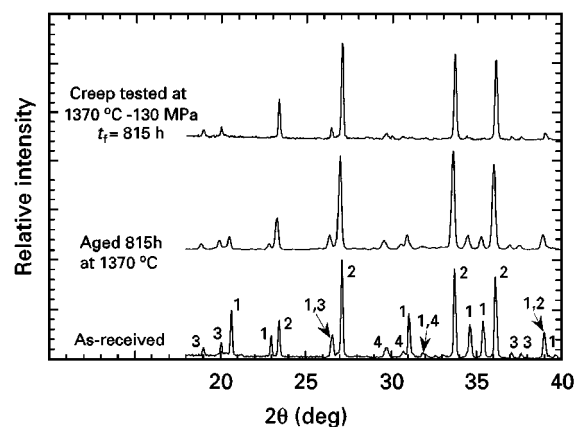


Figure 8 Comparing the X-ray diffraction profiles generated on materials that were creep tested at 1370 °C and aged at 1370 °C shows the  $\alpha$  phase content of the creep-tested material (stress and time) substantially decreased more than the material that was aged (time only). 1,  $\alpha$ - $\text{Si}_3\text{N}_4$  (9–250); 2,  $\beta$ - $\text{Si}_3\text{N}_4$  (33–1160); 3,  $\text{Si}_2\text{N}_2\text{O}$  (18–1171); 4,  $\alpha$ - $\text{Y}_2\text{Si}_2\text{O}_7$  (38–0223). The numbers refer to JCPDS card numbers.

appreciably. When the XRD profile for the 815 h aged specimen is compared to that for the creep-tested material (lifetime = 815 h) in Fig. 8, it is evident that the application of stress was associated with the further reduction in  $\alpha$  phase content. Like the aged specimens, the amount of secondary phase did not appreciably change. The results shown in Figs 7 and 8 reconfirm the observed trends in the  $\alpha$  to  $\beta$  transformation at 1370 °C from previous studies with  $\text{Si}_3\text{N}_4$  that were shown in Figs 1 and 4.

### 4.2.2. $\alpha$ to $\beta$ transformation kinetics

A first-order reaction utilizing Equation 2 [11] was found to represent the  $\alpha$  to  $\beta$  transformation quite well for the 1370 °C aged specimens. Being that the fraction of remaining  $\alpha$  could only be determined at 0 h and after creep rupture, only two datapoints were obtainable per creep test. A first-order reaction rate was used

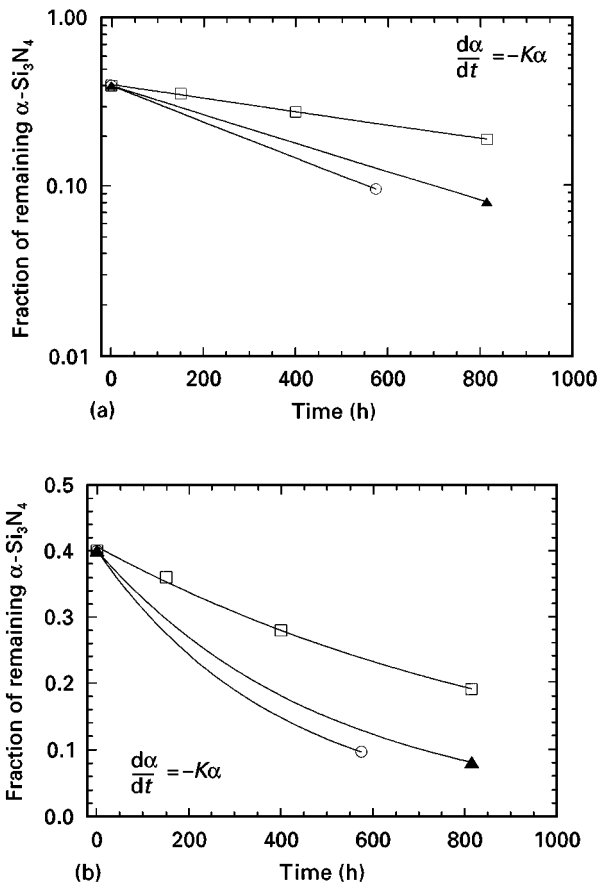


Figure 9 First-order reaction kinetics represented the  $\alpha$  phase reduction in the aged NT164 silicon nitride very well, and this is shown by the graphs having a logarithmic and linear ordinate axis in (a) and (b), respectively. Assuming this kinetic process represents the kinetics of the transformation during creep testing, the magnitude of the reaction-rate constant during creep testing at 1370 °C is twice that during ageing at 1370 °C. (a) ( $\square$ ) Aged (no stress)  $K = 0.00093 \text{ h}^{-1}$ , ( $\blacktriangle$ ) creep (130 MPa)  $K = 0.00198 \text{ h}^{-1}$ , ( $\circ$ ) creep (150 MPa)  $K = 0.00248 \text{ h}^{-1}$ . (b) ( $\square$ ) Aged (no stress), ( $\blacktriangle$ ) creep (130 MPa), ( $\circ$ ) creep (150 MPa).

to represent the change in remaining  $\alpha$  for the crept specimens, as was used for the aged specimens. The logarithm of the remaining volume fraction of  $\alpha$  phase was plotted on the ordinate axis as a function of linear time in Fig. 9a for the aged specimens and the high- $\alpha$ -containing specimens which were creep ruptured at 130 and 150 MPa. The slope (or reaction rate constant,  $K$ ) was determined to be  $0.00093 \text{ h}^{-1}$  for the aged  $\text{Si}_3\text{N}_4$  and  $0.00198$  and  $0.00248 \text{ h}^{-1}$  for the crept  $\text{Si}_3\text{N}_4$  specimens tested at 130 and 150 MPa, respectively. Here, a first-order reaction was assumed to represent the  $\alpha$  to  $\beta$  transformation with the application of stress, as it did for the aged material. As these results show, the  $\alpha$  to  $\beta$  transformation rate for the  $\text{Y}_2\text{O}_3$ -doped  $\text{Si}_3\text{N}_4$  examined in this study was stress dependent, which is consistent with behaviour previously observed in another silicon nitride [7]. The reaction rate constant was approximately 2 and 2.5 times as large for the crept material tested at 130 MPa and 150 MPa, respectively, than it was for the aged material. The temperature of 1370 °C is evidently high enough for the transformation of  $\alpha$  to  $\beta$  to occur, but the rate is quite slow. That is, the transformation occurs over hundreds of hours. A tensile stress

increases the rate. A greater stress increased it further, but the transformation still occurred over hundreds of hours.

The reaction rate of  $\alpha$  to  $\beta$  transformation varies from  $\text{Si}_3\text{N}_4$  to  $\text{Si}_3\text{N}_4$ . A linear-linear plot of remaining  $\alpha$  phase as a function of time is shown in Fig. 9b for the crept and aged NT164 materials. A comparison of Figs 1 and 9b shows that the  $\alpha$  to  $\beta$  transformation rate in NT154 and NT164 at 1370 °C is much slower than that in NCX-5102  $\text{Si}_3\text{N}_4$  for equivalent tensile stresses. Hundreds of hours were needed to halve the  $\alpha$  phase content in NT154 and NT164 at 1370 °C at stresses in the range of 130–150 MPa, while only tens of hours were needed for the  $\alpha$  phase content to be halved in NCX-5102  $\text{Si}_3\text{N}_4$  at an equivalent condition. NCX-5102  $\text{Si}_3\text{N}_4$  was developed to meet different goals of mechanical application (e.g. higher room-temperature strength [26]) than NT154 or NT164. The NCX-5102 material contains 4 wt %  $\text{Y}_2\text{O}_3$  as a sintering aid, as does NT154 and NT164. However, NCX-5102 was processed differently from NT154 and NT164 and contains aluminium which lowers the liquidus temperature of the secondary phases, which in turn may enhance the rapid transformation of  $\alpha$  to  $\beta$  [12]. It is acknowledged that the transformation rate of  $\alpha$  to  $\beta$  is dependent on several chemical and mechanical parameters, but the results in the present study confirm that stress is indeed one mechanical parameter that enhances the transformation rate at 1370 °C.

#### 4.2.3. Grain structure changes

In addition to the  $\alpha$  phase content changes, the grain structure of the NT164 also changed as a function of ageing time and the presence of stress. Representative microstructures of the plasma-etched polished surfaces for the as-received 40%  $\alpha$  phase material, the same material aged for 815 h, and the material that creep ruptured after 815 h are shown in Fig. 10a–c. The as-received microstructure in Fig. 10a shows the presence of small equiaxed grains mixed with more elongated grains, which are indicative of  $\alpha$  and  $\beta$  grains respectively. Some porosity is evident in Fig. 10a, but it is not known if this is indicative of residual porosity that resulted from processing the material, or if this constitutes grain pull-out from polishing. The secondary phase is fine-sized as well and is evident both at two-grain and multi-grain junctions. The XRD results for this as-received microstructure showed that 40%  $\alpha$  phase was present. After 815 h ageing, it is apparent from Fig. 10b that the grain structure changed; the amount of the fine-grain equiaxed grains evident in Fig. 10a appears to have lessened and the secondary phase appears to have segregated more to multi-grain junctions. The XRD results for this 815 h aged microstructure showed that the original 40%  $\alpha$  phase content had reduced to 19%. Lastly, the microstructure of the crept specimen that had a life of 815 h showed evidence of the most extensive grain coarsening, cavitation, and more extensive segregation of the secondary phase to multi-grain junctions, as shown in Fig. 10c. The specimen had

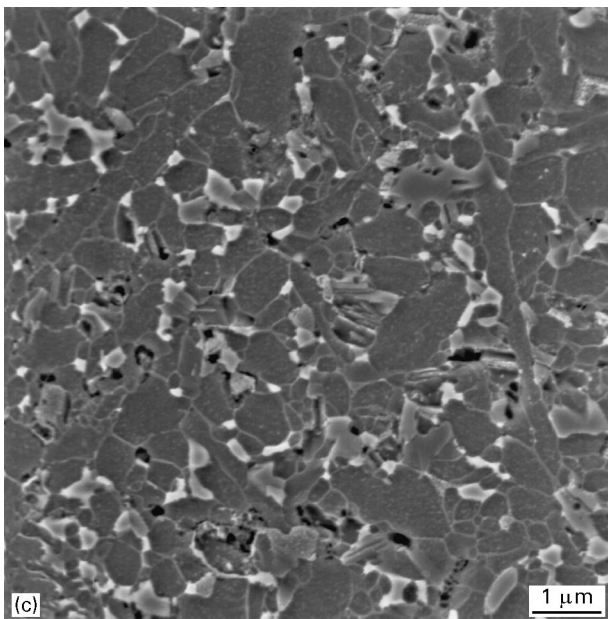
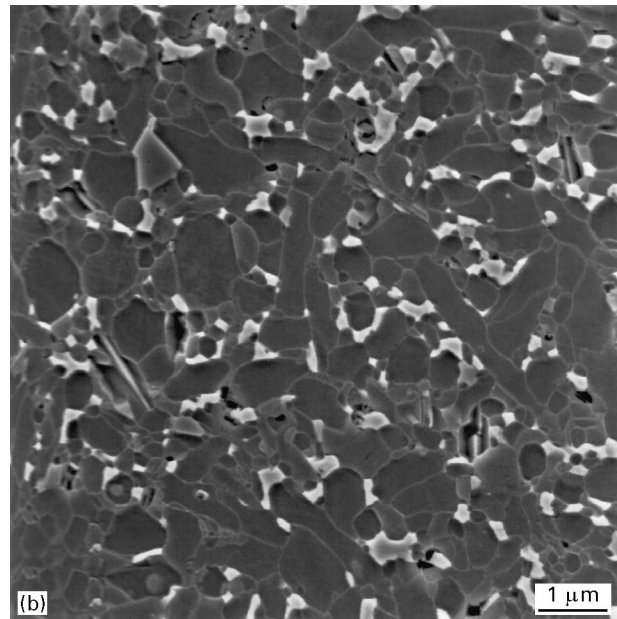
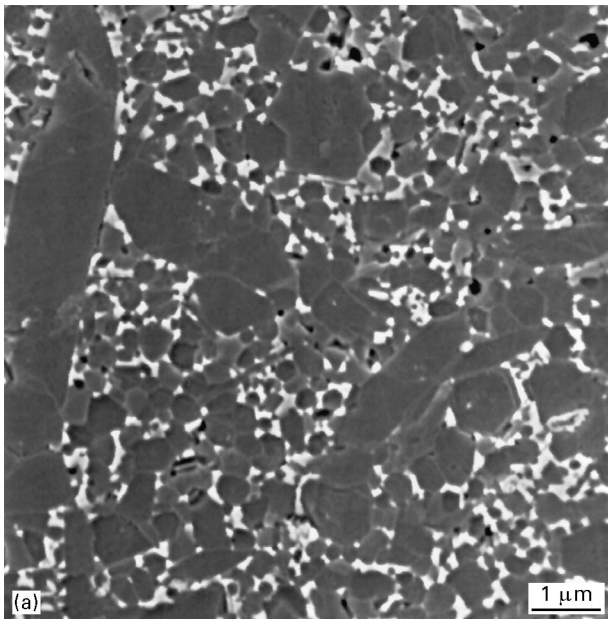


Figure 10 Plasma-etched polished surfaces and secondary electron imaging of the representative NT164 grain structure are shown for (a) the as-received material containing 40%  $\alpha$  phase, (b) the 40%  $\alpha$  phase grade material aged for 815 h at 1370 °C, and (c) the 40%  $\alpha$  phase grade material creep tested at 130 MPa and 1370 °C which had a lifetime of 815 h and creep strain to failure of 2.04%.

accumulated 2.04% of creep strain to the time of rupture and the multi-grain junction cavitation that is evident in Fig. 10c is indicative of this. The XRD results for this creep specimen's microstructure showed that the original 40%  $\alpha$  phase content had reduced to 8%.

It is evident that the reduction of the  $\alpha$  phase content is associated with the grain coarsening observed in the microstructures of materials that were aged or creep tested. Based on the discussion and the literature review of the  $\alpha$  to  $\beta$  phase transformation in Section 2, the small equiaxed grains of  $\alpha$ - $\text{Si}_3\text{N}_4$  likely dissolve at 1370 °C and do so more readily with the application of stress. The silicon and nitrogen species in the grain boundaries nucleate new  $\beta$ - $\text{Si}_3\text{N}_4$  or help grow existing  $\beta$ - $\text{Si}_3\text{N}_4$  grains, which causes the overall coarsening of the grain structure.

The improved creep resistance resulted from grain coarsening and greater intragranular interlocking as a consequence of the  $\alpha$  to  $\beta$  transformation. Interlock-

ing or pinning or equiaxed grains by networked, acicular grains is known to improve creep resistance [27]. In addition, an improvement in creep resistance is observed if the size of equiaxed matrix grains is increased in a material system in which the equiaxed grains are mixed with larger, acicular-shaped grains [28]. The presence of greater amounts of residual  $\alpha$ - $\text{Si}_3\text{N}_4$  was associated with poorer creep resistance because of the smaller overall grain size of this initial microstructure and the lack of grain interlocking. Thus, grain-boundary sliding could readily occur. This is an intriguing phenomenon because, in principle, creep resistance may be controlled or engineered by manipulating the phase state of the primary  $\text{Si}_3\text{N}_4$  grains which is quite different from manipulating the phase state of the secondary phases.

Although the presence of residual  $\alpha$ - $\text{Si}_3\text{N}_4$  was associated with poorer creep resistance, its initial presence in a component conceivably may be advantageous under special circumstances. For example, if a component made from virgin NT164 (with its high residual  $\alpha$ - $\text{Si}_3\text{N}_4$  content) is subjected to a high stress concentration in service (e.g. an intrinsic or extrinsic flaw, a high contact stress, etc.) then the poorer creep deformation associated with the presence of the  $\alpha$ - $\text{Si}_3\text{N}_4$  will be able to relax the stress in the volume of high stress concentration more efficiently than if the material was 100%  $\beta$ - $\text{Si}_3\text{N}_4$ . As the high stress concentration is relaxed, the  $\alpha$  to  $\beta$  transformation continues, and the creep resistance will improve over time as a consequence.

## 5. Conclusion

The creep resistance at 1370 °C (2500 °F) of yttria-doped, HIPed silicon nitrides increased as residual

$\alpha$  phase content decreased. For equivalent times and stresses, the silicon nitrides having a higher  $\alpha$  phase content accumulated more creep strain and exhibited a faster creep rate.

The greater creep resistance of the silicon nitride with higher  $\beta$  content was a consequence of more inhibited grain-boundary sliding due to the higher volume fraction of elongated grains. The poorer creep resistance of the higher- $\alpha$ -containing silicon nitride is associated with the small equiaxed geometry of the  $\alpha$  phase.

The  $\alpha$  to  $\beta$  phase transformation rate was found to be stress-enhanced at 1370 °C. The kinetics of the  $\alpha$  to  $\beta$  phase transformation at 1370 °C followed a first-order reaction in the absence of stress. If a first-order reaction was assumed for the  $\alpha$  to  $\beta$  phase transformation in the presence of stress at 1370 °C, then the magnitude of the reaction rate constant for this transformation was twice as large for tensile stresses equal to or greater than 130 MPa as the reaction rate constant describing the transformation with no applied stress.

### Acknowledgements

The authors thank A. E. Pasto and T. N. Tieggs for reviewing the manuscript and for their helpful suggestions, and P. F. Becher and H.-T. Lin for the use of their plasma etcher. Research sponsored by the Assistant Secretary for Energy Efficiency and Renewable Energy, Office of Transportation Technologies, as part of the High Temperature Materials Laboratory User Program, Oak Ridge National Laboratory, managed by Lockheed Martin Energy Research Corporation for the US Department of Energy under contract DE-AC05-96OR22464.

### References

1. D. CARRUTHERS and L. LINDBERG, in "Proceedings of the Third International Symposium on Ceramic Materials and Components for Engines", edited by V. J. Tennery, (American Ceramic Society, Columbus, OH, 1989) p. 1258.
2. M. K. FERBER and M. G. JENKINS, *J. Am. Ceram. Soc.* **75** (1992) 2453.
3. M. N. MENON, H. T. FANG, D. C. WU, M. G. JENKINS, M. K. FERBER, K. L. MORE, C. R. HUBBARD and T. A. NOLAN, *ibid.* **77** (1994) 1217.
4. A. A. WERESZCZAK, M. K. FERBER, T. P. KIRKLAND, K. L. MORE, M. R. FOLEY and R. L. YECKLEY, *ibid.* **78** (1995) 2129.
5. M. K. FERBER, M. G. JENKINS, T. A. NOLAN and R. L. YECKLEY, *ibid.* **77** (1994) 657.

6. A. A. WERESZCZAK and M. K. FERBER, unpublished results.
7. A. A. WERESZCZAK, T. P. KIRKLAND and M. K. FERBER, *J. Mat. Sci.* **31** (1996) 6541.
8. S. HAMPSHIRE, R. A. L. DREW and K. H. JACK, *Phys. Chem. Glasses* **26** (1985) 182.
9. S. M. WIEDERHORN and N. J. TIGHE, *J. Am. Ceram. Soc.* **66** (1987) 884.
10. D. R. MESSIER, F. L. RILEY and R. J. BROOK, *J. Mater. Sci.* **13** (1978) 1199.
11. L. J. BOWEN, R. J. WESTON, T. G. CARRUTHERS and R. J. BROOK, *ibid.* **13** (1978) 341.
12. P. DREW and M. H. LEWIS, *ibid.* **9** (1974) 261.
13. H. KNOCH and G. E. GAZZA, *Ceram. Int.* **6** (1980) 51.
14. D. R. MESSIER and W. J. CROFT, in "Preparation and Properties of Solid State Materials", Vol. 7 (edited by D.R. Messier and W.J. Croft, Marcel Dekker, New York, 1982) Ch. 2, p. 131.
15. L. J. GAUCKLER, H. HOHNKE and T. Y. TIEN, *J. Am. Ceram. Soc.* **63** (1980) 35.
16. N. R. OSBOURNE, G. A. GRAVES and M. K. FERBER, ASME Proceedings of the International Gas Turbine and Aeronautical Congress and Exposition, June 5-8, 1995, Houston, TX (ASME, New York, 1995).
17. V. M. PARTHASARATHY, J. R. PRICE, W. D. BRENTNALL, G. GRAVES and S. GOODRICH, ASME Proceedings of the International Gas Turbine and Aeronautical Congress and Exposition, June 5-8, 1995, Houston, TX (ASME, New York, 1995).
18. S. NATANSOHN, A. E. PASTO and W. J. ROURKE, *J. Am. Ceram. Soc.* **76** (1993) 2273.
19. A. TSUGE, K. NISHIDA and M. KOMATSU, *ibid.* **58** (1975) 323.
20. L. A. PIERCE, D. M. MIESKOWSKI and W. A. SANDERS, *J. Mater. Sci.* **21** (1986) 1345.
21. D. A. BONNELL, T.-Y. TIEN and M. RUHLE, *J. Am. Ceram. Soc.* **70** (1987) 460.
22. L. K. L. FALK and G. L. DUNLOP, *J. Mater. Sci.* **22** (1987) 4369.
23. A. E. PASTO, F. AVELLA, S. NATANSOHN and W. J. ROURKE, in "Silicon Nitride Ceramics, Materials Research Society Symposium Proceedings", Vol. 287, edited by I.-W. Chen, P. F. Becher, M. Mitomo, G. Petzow and T.-W. Yen (Materials Research Society, Pittsburgh, PA, 1993) p. 295.
24. D. J. DEVLIN and K. E. AMIN, *Powd. Diffract.* **5** (1990) 121.
25. C. CHATFIELD and H. NORSTROM, *Commun. Am. Ceram. Soc.* **66** (1983) C168.
26. V. K. PUJARI, D. M. TRACEY, M. R. FOLEY, N. I. PAILLE, P. J. PELLETIER, L. C. SALES, C. A. WILKENS and R. L. YECKLEY, "Development of Improved Processing and Evaluation Methods of High Reliability Structural Ceramics for Advanced Heat Engine Application, Phase I", US DOE Final Report, ORNL/Sub/89-SB182/1 (1993).
27. H.-T. LIN and P. F. BECHER, *J. Am. Ceram. Soc.* **74** (1991) 1886.
28. *Idem*, *ibid.* **79** (1996) 1530.

Received 28 January  
and accepted 17 December 1997